Front. Struct. Civ. Eng. 2024, 18(9): 1388–1400
https://doi.org/10.1007/s11709-024-1143-6

RESEARCH ARTICLE

An ultra-thin bolt tension sensor and online monitoring system: For application in hydropower plant unit

Shaoquan ZHANG[a], Yanke TAN[b*], Hanbin GE[a], Qilin ZHANG[b]

[a] *Department of Civil Engineering, Meijo University, Nagoya 4688502, Japan*
[b] *College of Civil Engineering, Tongji University, Shanghai 200092, China*
[*] *Corresponding author. E-mail: tanyk@tongji.edu.cn*

ABSTRACT The condition of bolted connections significantly affects the structural safety. However, conventional bolt tension sensors fail to provide precise measurements due to their bulky size or inadequate stability. This study employs the piezoresistive effect of crystalline silicon material to fabricate an ultrathin sensor. The sensor exhibits a linear relationship between pressure and voltage, an exceptional stability at varying temperatures, and a superior resistance to corrosion, making it adaptable and user-friendly for applications of high-strength bolt tension monitoring. A monitoring system, incorporating the proposed sensor, has also been developed. This system provides real-time display of bolt tension and enables the assessment of sensor and structural conditions, including bolt loosening or component failure. The efficacy of the proposed sensor and monitoring system was validated through a project carried out at the Xiluodu Hydropower Plant. According to the results, the sensor and online monitoring system effectively gauged and proficiently conveyed and stored bolt tension data. In addition, correlations were created between bolt tensions and essential unit parameters, such as water head, active power, and pressures at vital points, facilitating anomaly detection and early warning.

KEYWORDS ultra-thin sensor, high-strength bolt tension, online monitoring system, anomaly alarm, hydro-generator units

1 Introduction

High-strength bolts are widely used in the connections between structural members and professional equipment in the fields of water conservation, machinery, civil engineering, chemical industry, aerospace, and other fields. The safety of connected structures and equipment operations largely depends on the reliability of the bolted connections. The connected regions are inevitably subjected to mechanical and environmental effects (e.g., shock, vibration, and creep), and their long-term effects often lead to the loosening and sliding of each bolt, resulting in failure or even fracture of the bolt group connection, causing major engineering project accidents.

The monitoring of the tensile force of high-strength bolts and the corresponding damage detection is a branch that has received extensive attention in the field of structural health detection [1–3]. Many studies have been conducted to realize the tensile force monitoring of high-strength bolted connections. In terms of nonlinear dynamics, previous research analyzed and summarized the state monitoring and identification methods for mechanically bolted connections in detail [4]. Tong et al. [5] introduced the application of induced Lamb wave transformation and machine learning-based pattern recognition for online nondestructive monitoring on a joint steel plate. Wavelet analysis, a method focusing on both the time and frequency domains, has been proven to be efficient in identifying the structural parameters of bolted connections from the two-dimensional spectrum [6]. After the theory of the time reversal method was established, an increasing number of researchers began to infer the physical quantities that are not easy to monitor, including bolt preload according to the focused signal peak amplitudes [7,8], while the law of change between bolt surface roughness and monitoring accuracy was also discovered as auxiliary [8].

Article history: Received May 31, 2024; Accepted Jun 17, 2024

The author would like to divide the above trials into indirect methods that test the dynamic response of the bolted connection structure under input excitation during normal operation or in loosened cases, identify its dynamic parameters, and summarize the conditions of the bolts. The other category, direct methods, mainly consists of three branches: the fiber grating implantation method, piezoelectric method, and ultrasonic method. The fiber grating implantation method perforates the bolt and implants the fiber grating into the bolt hole with special structural glue to calibrate the relationship between the bolt stress and grating wavelength through the strain effect of the fiber grating [9,10]. Khomenko et al. [11] utilized a transducer embedded in a bolt shaft that allows quick assembly, disassembly, and reassembly to complete the preload and clamping force measurements. Additionally, a novel bending curvature sensor with an inextensible elastic matrix and offset grating was proposed by Deng et al. [12] to present the loosening angle of the monitored bolt.

In the beginning of this century, scholars developed a wireless prototype active sensor node for bolted connection preload monitoring, based on the impedance method [13]. The impedance method, a technology based on detecting changes in fixed piezoelectric device features, was experimentally studied by Wang et al. [14] to verify its performance in bolt-loosening detection tasks. These related sensors and methods were all built based on the fundamental relationship between mechanical and electrical parameters under the piezoresistive effect in germanium and silicon, which was revealed in the middle of the last century [15,16]. Recently, the frequency change of the piezoelectric impedance series was determined as another valuable indicator that can linearly reflect the fluctuation of the external pressure and therefore report the status of the bolts [17,18]. The principle of the piezoelectric method is that the material has positive and inverse piezoelectric effects. The measurement range depends on the compressive performance of the material, which is limited, resulting in a narrow application range for this method. In recent years, scholars have combined the piezoelectric effect with guided wave testing to determine the tension of a bolt by measuring the power of the guided wave and other parameters, thereby achieving active control [19–21].

Acoustoelastic theory describes the varying pattern between the velocity of elastic wave propagation in a stressed solid material and not only the material properties, but also the stress distribution [22]. Some scholars conducted theoretical research, measured the bolt tightening axial force based on ultrasonic technology, and made a preliminary prospect of the application field [23]. Similarly, the bolt axial force can be provided by a combination of changes in the length of the bolt and calibration constants, and the former part is measured by an ultrasonic extensometer operated by a mono-wave [24,25]. Amerini and Meo [26] monitored the bolted connection state and bearing torque by proposing a nonlinear index for the signal energy of the transmitted wave formed when the ultrasonic wave passed through the bolt. This method has high requirements for the geometry and physical state of the bolt and screw and requires a precise length of each bolt. The corrosion of materials or inconsistent temperatures will affect the data and hinder long-term monitoring missions.

Introducing richer information sources to grasp the conditions of bolts more precisely is another development direction in this field, which can be regarded as another type of indirect measurement method. Wang et al. [27] designed a real-time monitoring system for the bolt pretightening force based on IoT technology with powerful data mining and post-processing functions. From a mechanical perspective, the judgment of loosening or tightening the health state can be made by studying the relationship between the axial load and adjacent variables, such as displacement, acceleration, and strain of the local components of the flange [28,29]. For mass information collected from multiple sensors with complex internal correlation, neuron networks are suitable tools for analyzing [30,31]. Yuan et al. [32] used representative features extracted from multi-source data to train a convolutional neural to predict the tightness of the bolt connection structure. Xu et al. [33] introduced back propagation neural networks to extract information from data collected by electromechanical impedance and determined the bolt-loosening state for bolted spherical joints under different torque levels. However, the accuracy of machine learning-based methods is strongly affected by the training data set which can be noisy, partly missing, or even abnormal. Besides, these methods often have poor generalization performance when they are applied to another case. Thus, high-performance sensors are still in demand for both direct measuring and neural network training.

In this study, a varistor with a short physical length was used to develop an ultrathin high-strength bolt tension sensor. Simultaneously, an online monitoring system for high-strength bolt group tension was developed. In all areas where the results of this study are suitable, the turbine unit monitoring project of a hydropower station is representative. The entrance door of the hydropower station vibrates during the operation of the unit, which may cause the tightening bolts to loosen or break, reduce the prestress between the connecting parts, and finally disable the seal. Lacking locating the damage and warning in time may bring about the danger of tailwater backflow and flooding of the workshop. The top cover connecting the bolts is affected by temperature, stress, and vibration fatigue during the tightening process and long-term operation. Stress concentration was easily

encountered at the root of the bolt, resulting in fatigue cracks. Rapid expansion under the action of corrosion may lead to breakage of the bolts, thereby causing water leakage at the connection between the top cover and seat ring. In other words, the greater the hazard caused by bolted joint failure, the more necessary is a real-time, automated, and accurate monitoring system. With the modified sensors and the corresponding online monitoring system, the fluctuations, spikes, and trends occurring in the measured tension signals possess high synchronicity with the above-mentioned unit parameters, except for abnormal conditions. Thus, cross validation can be conducted to detect both plant anomalies and bolt loosening. The application of the proposed sensor and monitoring system was validated in this study to provide good technical support for ensuring the safe operation of the turbine unit of a hydropower station with a practical project in the Xiluodu Hydropower Plant.

2 Ultra-thin high-strength bolt tension sensor

With a brief introduction to the generic working theory of the pressure sensor, the production and manufacturing details of the proposed ultrathin high-strength tension sensor are presented in this section. The pressure-output voltage relationships of the proposed sensors with different shapes were calibrated, and their performance under varying temperatures was experimentally studied for applications.

2.1 Principle of pressure sensor

Monocrystalline or polycrystalline silicon has an obvious piezoresistive effect [15]. When these materials are subjected to mechanical stress, their resistance changes owing to the change in the carrier mobility, thereby causing the resistivity to change with a similar trend. Based on this phenomenon, a piezoresistive pressure sensor can be fabricated using a Wheatstone bridge structure. The pressure sensor contains three fixed-value resistors and one piezoresistor (R_1, R_2, R_3, and R_4), which are parallel to each other. The feeble output signals should pass through a filter to be denoised first and then detected and read out through a high-sensitivity voltmeter, as shown in Fig. 1.

When no stress was applied to the sensor, the four resistors exhibited a uniform resistance value, denoted as R. At this time, the bridge was balanced, and the readout of the pressure sensor was 0. Once pressure P is applied, the sensor film senses the external pressure and produces a corresponding stress change. The varistor, which is located in the area where the stress changes are most pronounced, will simultaneously experience a mutation in its own resistance. The Wheatstone bridge converts the change in resistance (ΔR) into an electrical voltage signal output by a voltmeter (V_{out}), which can be calculated based on a known input voltage (V_{in}) as

$$V_{out} = V_{in}\left(\frac{R+\Delta R}{R+R+\Delta R} - \frac{R}{R+R}\right) = V_{in}\frac{\Delta R}{4R+2\Delta R}. \quad (1)$$

The relationship in Eq. (1) allows us to determine the change in the resistance using the measured time series. Especially when ΔR is negligible to R, The equation can be further simplified to a linear relationship when ΔR is negligible. To obtain ΔR with high accuracy, V_{out} was amplified in the filter using a back-end signal processing circuit. On the other hand, the correlation between ΔR and P can be derived from the material properties of the varistor. However, instead of testing the material properties and theoretically establishing some correspondence with a large systematic error, it is better to acquire a calibrated relationship between P and V_{out} directly, ignoring all elements during the entire process.

2.2 Manufacturing and installation process

The proposed ultrathin high-strength bolt tension sensor

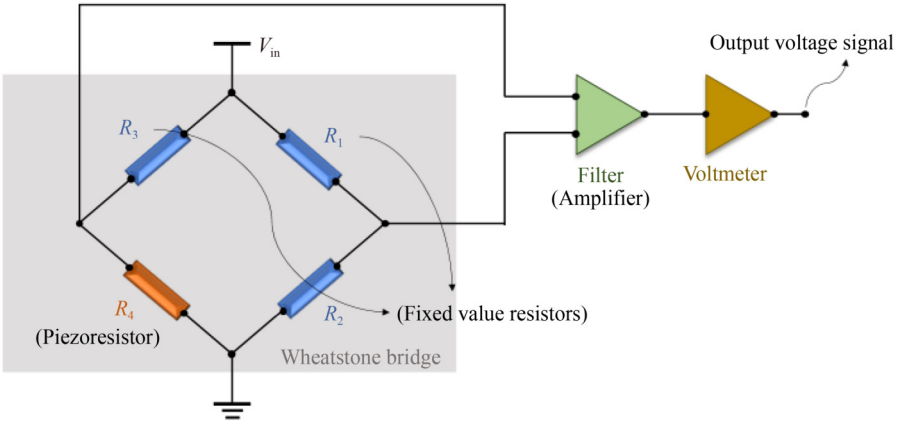

Fig. 1 Pressure sensor Wheatstone bridge circuit.

was developed based on the above theory. The proposed sensor is made into a ring shape, inserted into a high-strength bolt screw, and placed on the surface of the connected part. The tension sensor mainly consists of two components: an ultrathin varistor and a well-designed steel shell capable of protecting the circuit component and uniform load transmission. To improve the service life of the sensor and avoid uneven stress transmission caused by the uneven surface of the connected part and loosening caused by vibration, two gaskets were added to the upper and lower surfaces of the sensor (Fig. 2). When the bolt is installed, as the nut is tightened, tension begins to appear on the screw, and the sensor experiences equal pressure. After the feasibility and convenience of installation are guaranteed, two parameters must be determined to form an innovative sensor type, as introduced below.

In terms of materials, both high machinable flatness and high yielding strength are required for improvement. The former ensures that the pressure is transferred to the varistor uniformly to avoid stress concentration, whereas the latter provides a linear structural response within the entire measuring range of the tension sensor. 40CrMo alloy steel was selected through a comparison analysis of No. 45 steel. The final machinable surface planarity of steel No. 45 is unacceptable. The results of the material tests show that steel No. 45 has a high possibility of creating drift failure of acquisition data due to local stress concentration caused by material inhomogeneity (the corresponding strength is approximately 200 MPa), while the 40CrMo alloy steel has a relatively higher yield strength, which causes plastic deformation and failure of the sensor when the pressure is increasing (the corresponding strength is higher than 900 MPa). Tension is transmitted to the varistor only when the sensor shell is in the elastic stress stage. Once the shell undergoes a large plastic deformation, the force transmission path will change accordingly, and finally, the load sensed on the varistor will change, causing errors. Especially in dynamic monitoring tasks, irreversible shape changes make all subsequent monitoring results unreliable.

In contrast, the conventional size of the varistor used in traditional pressure sensors is 30 mm, and two balance segments with lengths of 30 mm are required at both ends of the varistors to equalize the stress. Together with the installation space for the varistor, which was at least one-third of the sensor length, the minimum thickness of the sensor was determined to be 100 mm. A limitation of the traditional sensor is that it is too thick to be used in high-strength bolts with short screws. After the tests, a 3 mm length varistor from Kyowa was selected with a well-designed coat for bearing and heat insulation, the shape of which is shown in Fig. 2. This brand of resistor effectively reduces the thickness of the pressure sensor to a uniform 10 mm regardless of the diameter of the bolt monitoring, whereas the thickness of the traditional sensors depends on the target geometry and measuring range.

2.3 Pressure-output voltage relationship calibration

Calibration experiments were carried out for the two shapes of the proposed pressure sensors with inner diameters of 30 and 100 mm, respectively. A cyclic load was applied to each pressure sensor specimen three times using a universal amplitude (240 kN for the small-sized specimen, and 1500 kN for another) to verify the repeatability. The adopted hydraulic servo press is shown in Fig. 3(a), which can also provide an inline load, while the output voltage is collected by the voltmeter installed on the acquisition device after the signal adapts to the current load of each loading step. During this test, the excitation voltage was set at 5 V.

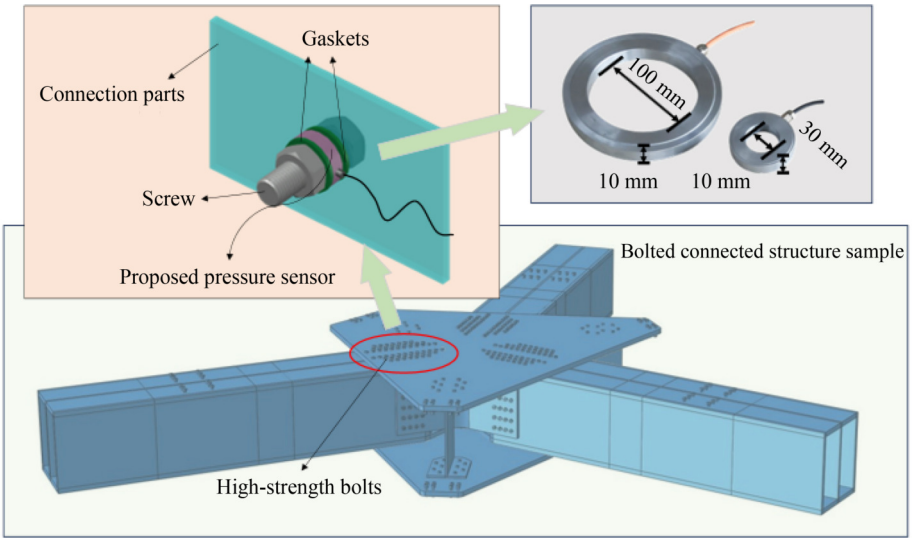

Fig. 2 Installation of the proposed sensor.

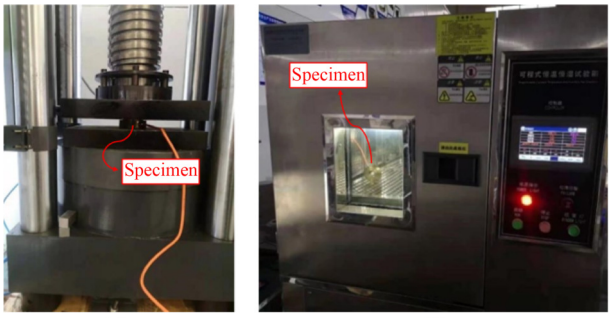

Fig. 3 Testing equipment: (a) loading press; (b) constant temperature box.

The voltage-pressure curves for the two groups of tests with different dimensions are shown in Figs. 4(a) and 4(b), respectively. In general, the results of the two groups of tests indicate that the proposed sensor has a high stability for monitoring varying pressures in different ranges. The data measured from the sensor with a large diameter had a larger dispersion, which may be caused by uneven compression or the applied load being close to the upper limit of the press. In other words, a sensor with a smaller diameter has a more reliable readout under dynamic loads within its measurement range. More importantly, the relationship between pressure and output voltage was almost linear. Thus, the fitting lines obtained by the least-squares method are also plotted in the figures. The two fitting lines have smaller intercepts than the entire testing range (under 5%); therefore, they can be regarded as lines close to the approximate straight line through the origin. The overall slope of the fitting line of the sensor with a larger diameter is nearly four times that of a smaller diameter, whereas its initial slope is relatively lower, revealing that there is a non-obvious turning point in the relationship when the pressure is approximately 300 kN. However, the slope change was negligible, and we used a linear calibration relationship for the proposed sensor.

2.4 Temperature performance test

The pressure sensor regularly calculates the pressure by sensing the stress changes on the film; however, in practical applications, mechanical forces can cause stress. The deformation of the metal shell and the change in the mechanical properties or resistance performance of the resistor itself caused by the temperature change may lead to inaccurate final output voltage signals [34]. Therefore, in addition to the temperature performance test of the sensor during the sensor development stage, in actual projects, a thermometer is often installed around pressure sensors or strain gauges to eliminate the influence of temperature. For the proposed sensor, considering only one standard geometry (inner diameter of 100 mm and thickness of 10 mm), a series of temperature tests was conducted in a constant-temperature test box (Fig. 3(b)). The test range was 0 to 60 °C with a step size of 5 °C. A temperature holding process lasting for 10 min was added between each of the two heating steps to ensure that the sensor reached the indicated temperature. The heating process was repeated thrice, and the output voltage was recorded after the stabilization of each step. During this test, the excitation voltage was set at 12 V. The results are shown in Fig. 5.

The average standard deviation of the output voltage for the three tests is 0.49 mV, which is not significant compared to the design varying range. Especially for the second and third trials, the output voltage fluctuates only from −112 to −109 mV, indicating that the proposed sensor has high temperature stability. Even in the second and third trials, where an upward trend can be observed at the end of the heating process, within the commonly used temperature range (lower than 50 °C and greater than 10 °C), the amplitude of this drift is less than 0.2 mV, which has a negligible impact on the monitoring of bolt tension. Therefore, we can use a constant value to represent the influence of temperature on the sensor. And

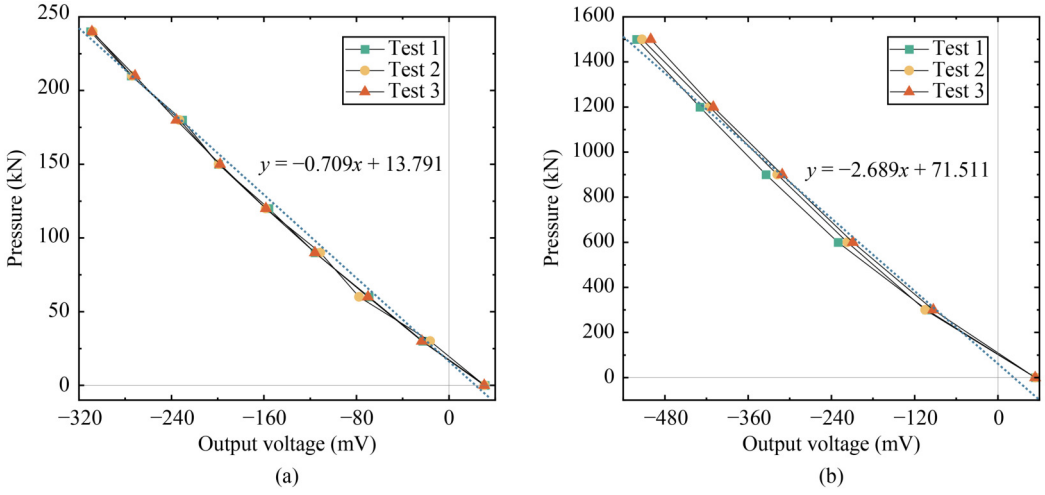

Fig. 4 Calibration curves for two shapes of proposed sensors: (a) diameter of 30 mm; (b) diameter of 100 mm.

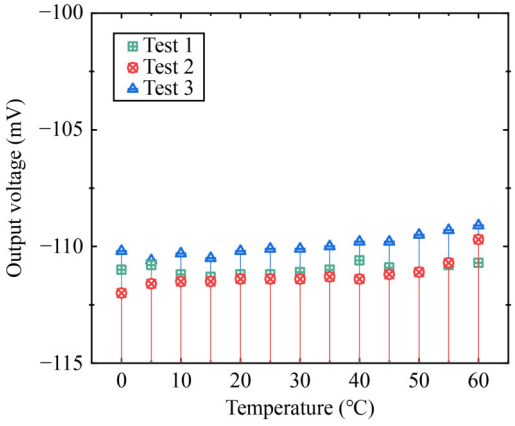

Fig. 5 Temperature performance of the proposed sensor.

then, we can compensate the output tension data by just deduct the force aroused by this stable voltage value. In addition to the cases with a small fluctuation range, there is no need for adjacent temperature sensors for calibration.

3 High-strength bolt tension online monitoring system

In this section, we will develop a monitoring system that works with the proposed novel bolt tension sensor, which has the functions of measuring, assessing, and controlling. The architecture of the system is briefly introduced, and the data processing and evaluation processes are illustrated in detail.

3.1 Monitoring system architecture

The high-strength bolt tension online monitoring system consists of four parts: sensor array, data acquisition and transmission network, data processing and control terminal, and performance evaluation model. The system structure is illustrated in Fig. 6. The group of bolt-tension sensor elements is the front-end part of the monitoring system, which is responsible for accurately collecting tension information and converting it into electrical signals. The network system of the second part, comprising several parallel acquisition instruments that connect sensors through their individual channels, can transmit analog signals collected from the sensors into digital signals and pass them to the processing equipment wirelessly. The sensors were grouped and connected to the distributed acquisition devices through a bayonet nut connector to avoid long-distance routing. An Accurate IoT Explorer high-speed automatic acquisition instrument was chosen for the system, which is small in size and highly integrated. This acquisition equipment is suitable for long-term automatic monitoring, and its maximal sampling frequency is 1000 Hz, which is sensitive to any frequency component of signals from the field of structural engineering.

The measurement information was preliminarily processed and analyzed in the third subsystem. We employed Lenovo SR530 as the servers that are directly connected to the switch (S5720-28P-SI). The selected real-time varying curves of the bolt tensions are dynamically displayed via visualization software on a high-performance server, whereas the rest are stored in the mass data storage equipment. According to the monitoring data of bolt tensions, determining the performance of the bolt group and providing early warning, if necessary, are the final functions of the proposed system. At the same time, this system also has data interfaces with other external data-processing

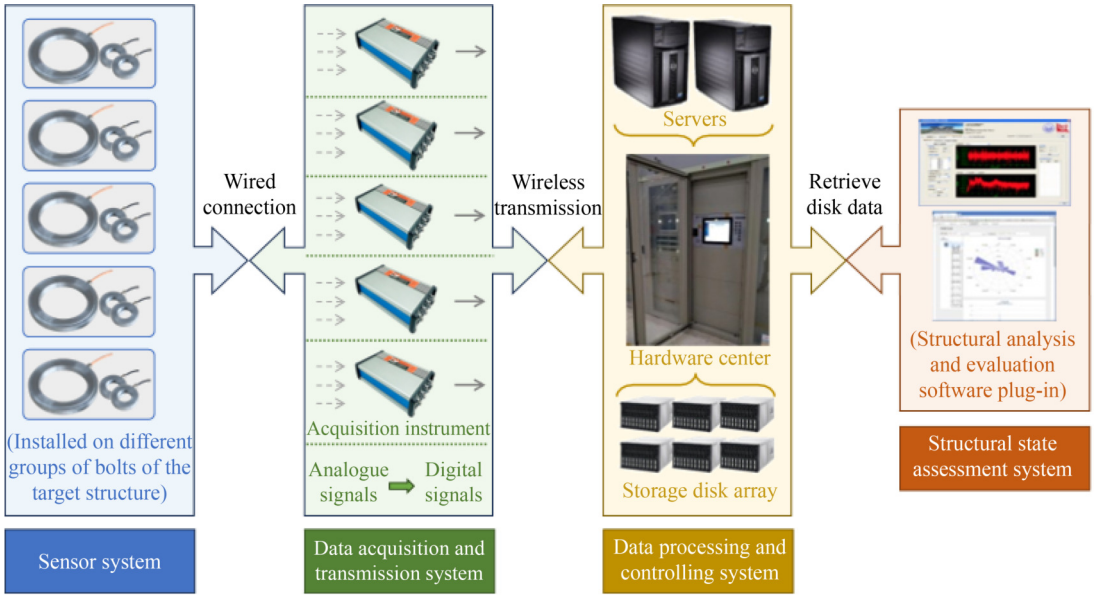

Fig. 6 Architecture of the online monitoring system for high-strength bolt tension.

software. Compared with the traditional monitoring system, the automatic monitoring system in this study has five advantages: accurate and efficient data acquisition, timely data visualization and analysis, convenience of storing and recalling massive amounts of data, quick feedback of risk information, and real-time remote access to bolt status.

3.2 Data processing and evaluation modules

The hardware of the data processing and control system consists of high-performance servers with large-capacity storage disk arrays. Simultaneously, a hardware firewall was installed to ensure the safety partition requirements of practical projects. The automatic monitoring and behavior evaluation software platform (consisting of plug-ins for image generation, structural analysis, state assessment, and risk warning) is deployed on the server, and terminal devices such as mobile phones, computers, and tablets can be used to log into the system to access the software platform to realize basic operations such as query, modification, export, summary, and printing of automatic monitoring data. The detailed functions of the platform are listed in Table 1 and some of the interfaces are shown in Fig. 7.

4 Case study

The feasibility and superiority of the proposed sensor and the corresponding monitoring system will be validated by applying it to a practical project (Xiluodu Hydropower Plant). The sensor installation and system establishment processes are described in this section, and the measurement results are also provided. Subsequently, we determined the scope of application, advantages, and limitations of the proposed technology.

4.1 Xiluodu Hydropower Plant and its monitoring arrangement

Xiluodu Hydropower Plant is a key project of “West-to-

Table 1 Functions of software platform in the proposed monitoring system

Module	Function	Note
Project management	project information editing	create, delete, and name projects; enter and modify project full-cycle information
	user rights setting	create and delete user accounts; initialize passwords; assign permissions of using software, project information, and historical data
Acquisition management	acquisition instrument management	create, delete, name, and number acquisition instruments; set measuring parameters (sampling frequency, sensitivity, compensation value, etc.)
	sensor management	create, delete, name, and number sensors; set sensor types and parameters; edit sensor calculation formulas; set sensor connection diagram
	measuring point management	create, delete, name, number, and locate measuring points; associate measuring points with sensors
	acquisition controlling	establish communication to acquisition instrument; start and stop acquisition remotely; set data transmission method and storage location
Data processing management	data writing	store measured data automatically; enter user-defined data manually; combine data from different sources
	statistical analysis	summarize database according to time (weekly, monthly, or yearly) and location; calculate statistical parameters for variables (means, variances, covariances, and correlation coefficients)
	time-frequency domain analysis	conduct time series analysis in time or frequency domains; identify structural parameters and modes
Display management	measuring data real-time display	real-time display of tension changes at each measuring point based on latitude and longitude coordinates
	diversified display of analyzed data	diversified display for current and historical signals with the corresponding calculated parameters; modify image and table parameters (appearance style, axis, title, etc.)
Risk warning management	warning rule setting	enter warning rules based on related standards or previous researches; set warning ranges, thresholds, levels, and displaying methods
	warning log recording	automatically generate, store, and sort warning logs; record abnormal data and measures taken during the whole warning process

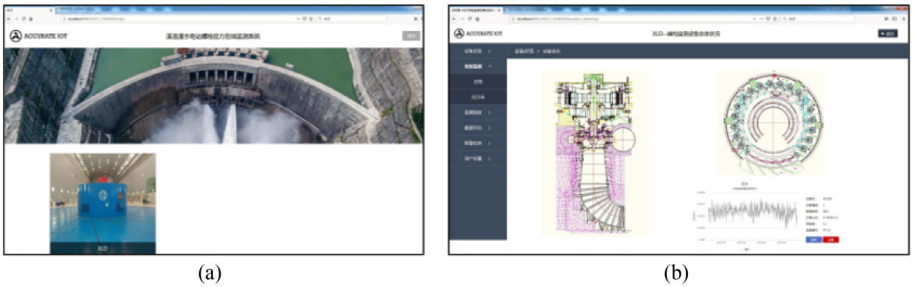

(a) (b)

Fig. 7 Interfaces of the software platform: (a) project management module; (b) displaying management module.

East Power Transmission" project of China. The project mainly focuses on power generation and has comprehensive benefits, such as flood control, sand retention, and improvement of upstream shipping conditions. The hydro-generator unit is mainly composed of high-strength bolt groups, which experience dynamic loads during the entire operation process and face the risks of loosening and slipping. In addition, the large number of complex-shaped components in the hydro-generator unit significantly limits the length of the screw, which in turn places higher requirements on the thickness of the sensor. Thus, an ultrathin bolt tension sensor and a corresponding monitoring system are urgently needed.

Eight high-strength bolt tension sensors were arranged in the bolt group of the hydro-generator unit. Two M100 bolts were measured at the top cover plate and seat ring, two M30 bolts at the volute door handle, and four M30 bolts at the door handle of the taper pipe (Figs. 8(a)–8(d)). The bolts of two sizes are measured by the proposed sensors whose inner diameters are the same as those of the screw diameters; that is, the sensors that are used to conduct calibration in Section 2. On-site installation includes sensor installation, pipeline and cable laying, and system commissioning. The uniform sampling rate for all sensors was 100 Hz to ensure clear monitoring of sudden events such as impacts, fractures, and dynamic failure of the rock mass. After the sensors and system equipment were installed, a system debugging operation was performed. Three collection boxes were fixed to the volute door, cone door, and top cover to link the sensors of each group. The sensors send the bolt tension data to the switch and server located in the factory hall through the collection box, and finally to the office area under the firewall. Subsequently, real-time viewing and analysis can be realized. It is worth mentioning that the lengths of the bolts at the top cover, volute, and cone door are limited by the environment of their location and considering the minimum thickness of the nut and gasket, the requirement for sensor thickness is extremely high. The traditional bolt tension sensor is not suitable here, and the advantages of the ultrathin (10 mm) high-strength bolt tension sensor proposed in this paper can be brought into play.

4.2 Application results

4.2.1 Construction of the proposed sensors

According to the design requirements, the torque method was employed to pre-tighten all the high-strength bolts of the hydro-generator unit. Bolt groups with the same design load-bearing capacity adopted a uniform installation torque to achieve the same degree of pre-tension. The M30 bolts were screwed with an electric wrench and the M100 bolts were screwed with a hydraulic wrench, as shown in Figs. 9(a) and 9(b). The bolts installed with the corresponding sensors are shown in Figs. 9(c) and 9(d).

However, the torque method encounters obstacles in practical operation; that is, the torque applied to each bolt will not be translated equally to tension on the corresponding screw, causing discreteness that cannot be ignored. This is mainly due to the divergence of the contacting surface parameters, which are influenced by the materials of the bolts and components to be connected, surface treatment methods of the contacting parts, environmental humidity, and use of lubricating oil. In general, the rougher the contact surfaces, the more energy applied by the torque is dissipated by friction instead of being converted into the potential energy of the bolts. The role of the pressure sensor installed synchronously with the bolt is highlighted, with the online data stream collected by, which serves as a reference to improve the reliability of the installation process. First, the installer can fine-tune the torque based on the real-time readings output by the pressure sensors to ensure that the pre-tightening forces of the bolts satisfy the design requirements. Second, with a uniform pressure sensor and its gaskets as a buffer, the discreteness caused by the surface roughness of different materials can be

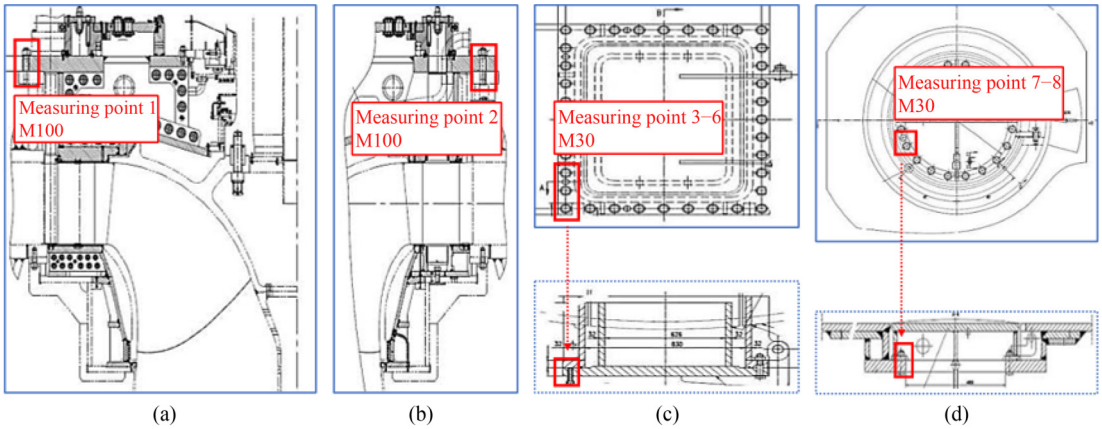

Fig. 8 Measuring point arrangement: (a) top cover; (b) seat ring; (c) volute door; (d) cone door.

Fig. 9 Construction process of sensors and bolts: (a) pre-tightening of M30 bolts; (b) pre-tightening of M100 bolts; (c) installed M30 bolts with sensors; (d) installed M100 bolts with sensors.

greatly reduced. Third, based on the discreteness being effectively limited, we can calibrate the relationship between the real tension output by the sensor and the applied torque to facilitate the installation of other bolts that do not have a pressure sensor and have similar working conditions. Considering that lubricating oil has a strong impact on the coefficient of friction between the gasket and other materials, we calibrated the two cases of using and not using lubricating oil separately and obtained the data listed in Tables 2 and 3. The torque coefficient was defined as the ratio of the real bolt tension to the applied torque. This parameter builds the end-to-end relationship between the readouts and target, and thus can be used to guide the installation of other sensors.

The same M30 bolt was calibrated by tightening it three times before and after the addition of lubricating oil. Evidently, the conversion rate of torque to bolt tension increases after lubricating oil is applied, and because the lubricating oil smooths out the roughness difference caused by the materials, the variance of the torque coefficient obtained by the second set of calibrations is also reduced. The torque coefficient is calculated by dividing the measured bolt preload by the torque, which can be used to quickly acquire the actual preload of adjacent bolts under similar conditions under a certain torque.

Table 2 Relationship between bolt tension and applied torque (without lubricating oil)

Torque (kN·m)	First trial		Second trial		Third trial	
	Voltage (mV)	Tension (kN)	Voltage (mV)	Tension (kN)	Voltage (mV)	Tension (kN)
0	34	0	34	0	35	−0.5
440	−56	45	−137	85.5	−163	98.5
700	−177	105.5	−232	133	−230	132
1000	−297	165.5	−361	187.5	−314	174

Torque coefficient of the first, second, and third trial are 0.166, 0.188, and 0.174, respectively.

Table 3 Relationship between bolt tension and applied torque (with lubricating oil)

Torque (kN·m)	First trial		Second trial		Third trial	
	Voltage (mV)	Tension (kN)	Voltage (mV)	Tension (kN)	Voltage (mV)	Tension (kN)
0	38	0	38	0	37	0.5
440	−168	103	−186	112	−206	122
600	−256	147	−268	153	−264	151
1050	−369	203.5	−382	210	−374	206

Torque coefficient of the first, second, and third trial are 0.194, 0.200, and 0.196, respectively.

4.2.2 Monitoring results during operation

After the installation of both sensors and the monitoring system, the bolt tension data will be collected and passed to the storage equipment. To obtain valuable information from the massive data and then determine the status of the bolts and connected structure, the potential correlations between the bolt tension and other working parameters of the hydro-generator unit should be studied first.

Figure 10(a) shows the time series of the bolt tension and unit water head, which represent the water-passing ability of the hydropower station. There was a relatively strong positive correlation between the two variables. This means that the higher unit water head tends to disengage the components connected by bolts, and thus, the pressure in the screw increases. The positive correlation is further indicated by Fig. 10(b), which is plotted by the gradients of the two variables. Additionally, according to Bernoulli's principle, the velocity behind the gate is significantly influenced by the water head of the unit and exhibits a similar varying trend (Figs. 11(a) and 11(b)). Thus, we can also discover a positive correlation between bolt tension and velocity after the sluice.

Furthermore, the pressures of the taper pipe inlet and end of the volute are two entities that are commonly used to identify the conditions inside the hydro-generator unit. Figures 12(a) and 12(b) illustrate the corresponding curves. Regardless of some local fluctuations, the bolt tension and pressure at the inlet of the taper pipe exhibited a reverse trend. This means that the pressure at this location causes the two members of the bolted connection to come close to each other. However, the pressure at the end of the volute is an obtuse variable, whose trend tends to be slow. In particular, when the bolt tension fluctuates within a small range around a certain value, the pressure at this location is almost constant. Only when the bolt pressure rises or falls to another level will it slowly change to the next platform, resulting in the shape of its signal being stepped. However, the pressure at this location is a sensitive variable that reflects the change in the bolt tension. For the two sudden drops in bolt tension during the measurement period, two synchronous jitters can be observed.

During the three-day monitoring period, the hydro-generator unit was turned twice: at 18:00 on December 24 and 16:00 on December 25, 2018. This can be verified from the active power of the generator unit and PC5 rotational speed signals. These two moments almost coincide with the abrupt change in bolt tension, as shown in Fig. 13. In other words, this correspondence, as well as the results obtained in Figs. 10–12, can be used to verify whether the bolts and components of the unit are abnormal. The appearance of asynchronous outliers in only one signal indicates that the corresponding position may be damaged or malfunctioned. This is the principle

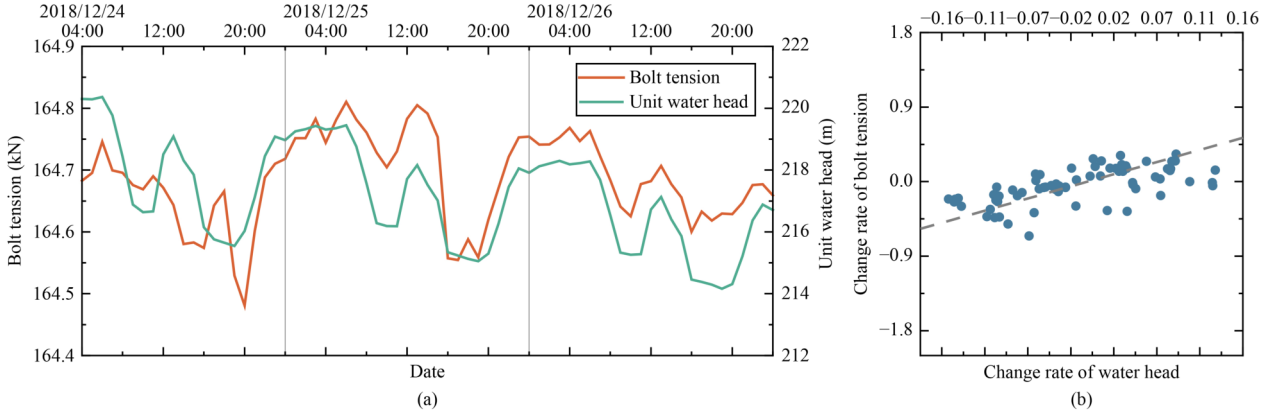

Fig. 10 Relationship between bolt tension and unit water head: (a) comparison between bolt tension and unit water head; (b) correlation of gradients.

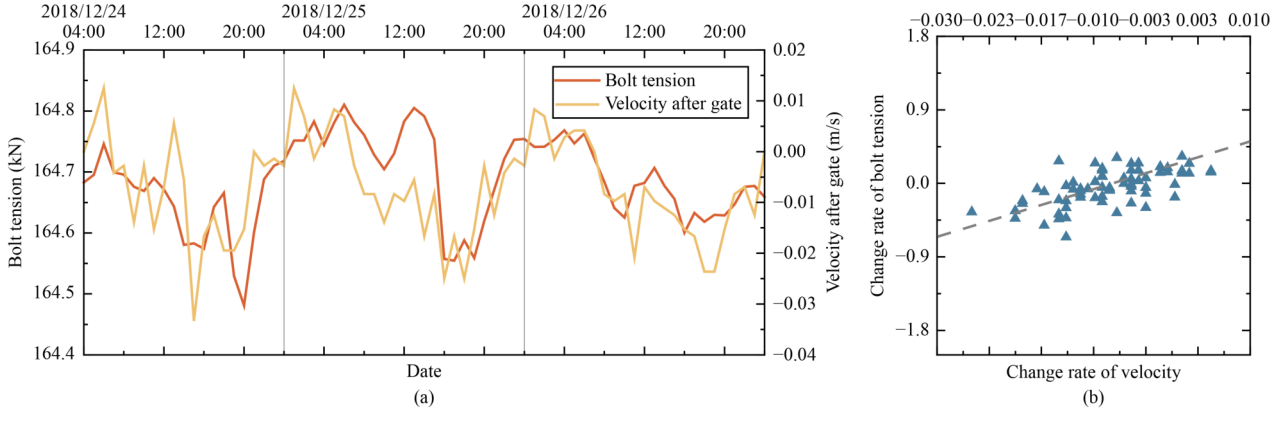

Fig. 11 Relationship between bolt tension and velocity after gate: (a) comparison between bolt tension and velocity after gate; (b) correlation of gradients.

that bolt tension data can be used for structural state assessment and damage identification and is also necessary for this detection work. However, this mutual detection method is only suitable for variables that have a mechanical causal relationship with bolt tension. For variables such as water levels behind the fast door and sluice (Fig. 14), it is difficult to predict them, and it is also difficult to infer the bolt status by them. In summary, for other monitoring quantities that can affect bolt tension, in addition to its own empirical or theoretical state evaluation criteria, the data returned by the proposed ultrathin high-strength bolt tension sensor can also be regarded as an effective supplement for the structural working state.

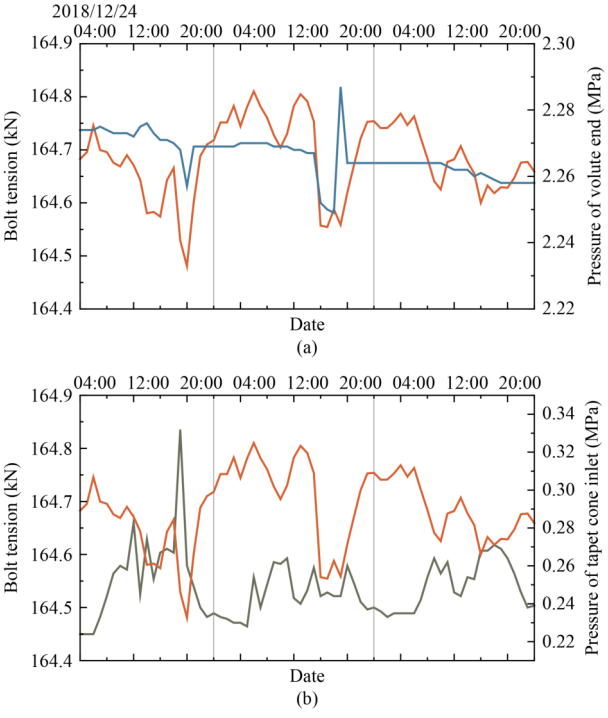

Fig. 12 Relationship between bolt tension and component pressure: (a) comparison between bolt tension and cone pressure; (b) comparison between bolt tension and volute pressure.

4.3 Other application, limitation, and future work

In addition to the above-mentioned Xiluodu Hydropower Plant, ultra-thin high-strength bolt tension sensors and the corresponding real-time online monitoring systems have been successfully applied to the Beijing Xinshougang Bridge (a bridge across the Yongding River), Jiashao Bridge, Yancheng Dafeng Offshore Wind Power Station (300 MW), Nanjing Hongyang Plaza complex curved roof, etc. In addition to effectively obtaining real-time data and conducting safety assessments for the target structure and its high-strength bolts, we found that there is still optimization work for the sensors and monitoring system proposed in this paper. For the proposed sensor, independent calibration was required for every sensor size determined by various bolt dimensions. Thus, a model based on experimental data to predict the bolt tension-output voltage relationship based on the material and geometric parameters is required in the next stage of research. For the monitoring and assessment system, the damage detection result for a certain location in the present version of the algorithm was calculated using the data collected from the nearest sensor. However, one individual sensor can be easily influenced by noise, whereas other sensors that are not far away from the concerned location are also valuable. Thus, a data-fusion-based algorithm for combining structural information hidden in different signals is also one of our future works, whose accuracy will be foreseeably higher.

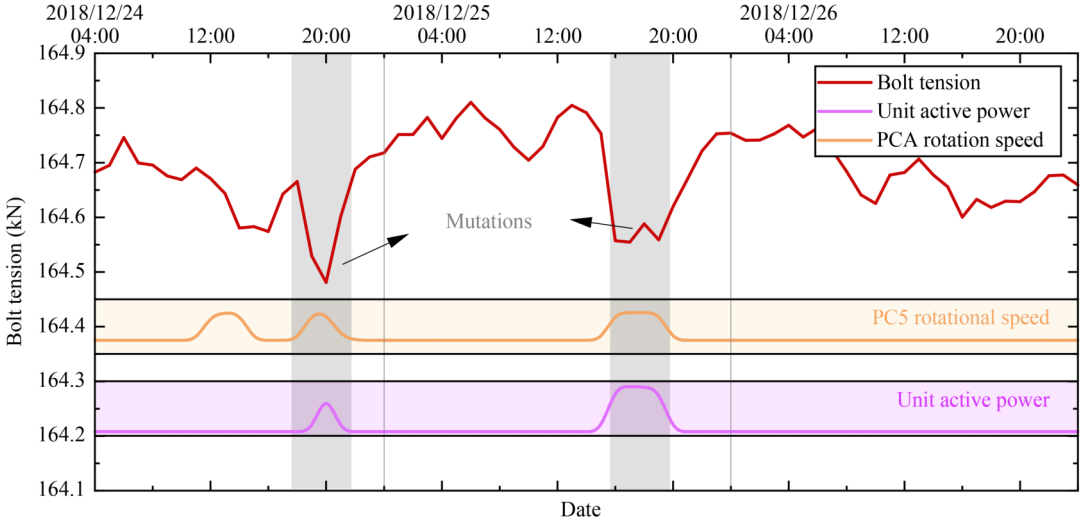

Fig. 13 Relationship between bolt tension and unit working state.

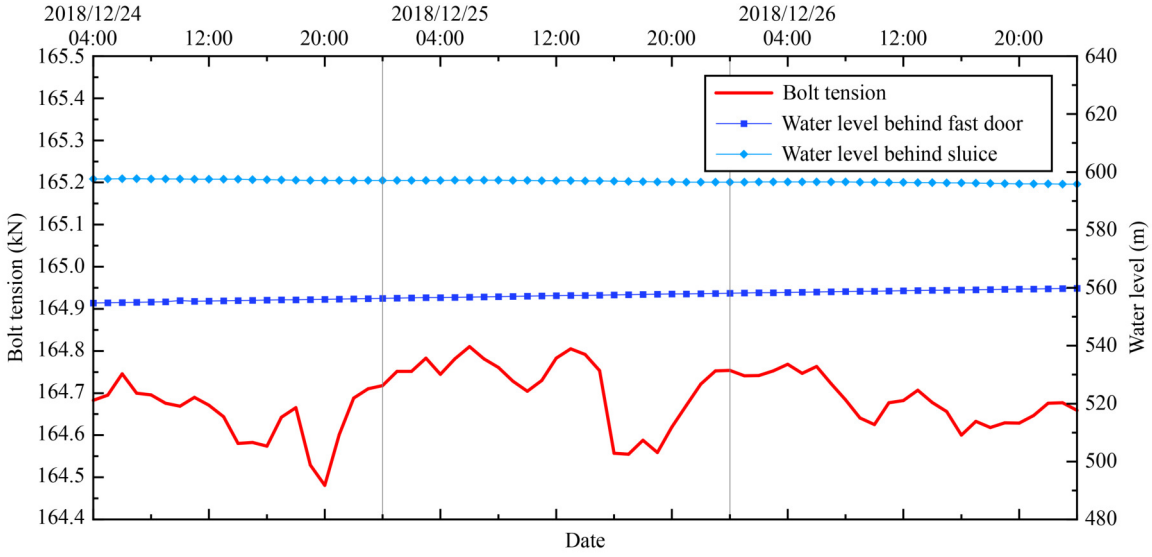

Fig. 14 Variables without relevance to bolt tension.

5 Conclusions

In this study, an ultrathin tension sensor was proposed for detecting the screw tension of high-strength bolts. The sensor shape and material were optimized for higher performance based on experimental studies. A real-time monitoring system for collecting, transmitting, visualizing, and digging bolt-tension data was also developed. The superiority of the proposed sensor and monitoring system was verified by a practical project at a hydropower plant. The following conclusions can be drawn.

1) The ultrathin tension sensor has applying priority in complex conditions owing to its lower spatial occupation of installation and operation (thickness: 10 mm). The calibration tests show high repeatability and multiple arrangement convenience. In addition, a standard deviation of only 0.49 mV is observed in the temperature tests which allows us to use uniform parameters to stably eliminate temperature effects, broadening the scope of application of the sensor.

2) The proposed sensor, sandwiched between the nut and structural members, reduced the discreteness of the friction coefficient of the contacting surfaces. The readouts of the sensor cannot only be used to meet the preload requirements of the bolt more accurately (torque coefficients: 0.176 (with surface lubrication) and 0.197 (without surface lubrication)) but also can be regarded as the tightening reference of other bolts under the same working conditions.

3) The proposed monitoring system can display the tension of bolts on the target structure in real time and in various effective ways. In addition, the bolt tension has the same variation trend as the water head of the unit and the flow velocity behind the gate and has the opposite variation trend with the inlet pressure of the tapered pipe. The correlations can be used to detect the bolt working status and provide an alarm, if necessary.

4) The action power of the unit, PC5 rotational speed, and pressure at the end of the volute are inert in fluctuating, but sensitive to bolt tension mutations owing to the unit startup and shutdown. Thus, asynchronous sudden changes (100 r/min and 500 W) provide valuable information for detecting anomalies and damage in structures connected by high-strength bolts.

In addition to further improving the accuracy and data transmission capabilities of the sensors and their monitoring system, the future work of this study should focus on automated data processing algorithms. We plan to develop a data-driven bolt loosening detection algorithm. Furthermore, a main structure condition assessment method using bolt tension data will be proposed based on an in-depth study of the mapping relationship between bolt tension and important parameters of the main structure.

Competing interests The authors declare that they have no competing interests.

References

1. Rehman S, Usman M, Toor M, Hussaini Q A. Advancing structural health monitoring: A vibration-based IoT approach for remote real-time systems. Sensors and Actuators. A, Physical, 2024, 365: 114863
2. Song G, Li W, Wang B, Ho S. A review of rock bolt monitoring using smart sensors. Sensors, 2017, 17(4): 776
3. Wang T, Song G, Liu S, Li Y, Xiao H. Review of bolted connection monitoring. International Journal of Distributed Sensor Networks, 2013, 9(12): 871213
4. Huang J, Liu J, Gong H, Deng X. A comprehensive review of loosening detection methods for threaded fasteners. Mechanical

Systems and Signal Processing, 2022, 168: 108652
5. Tong T, Hua J, Gao F, Lin J. Identification of bolt state in lap joint based on propagation model and imaging methods of Lamb waves. Mechanical Systems and Signal Processing, 2023, 200: 110569
6. Yan H, Zeng G, Zhao D, Tian M. Fault diagnosis of the attachment bolt looseness based on wavelet analysis. Mechanical Science and Technology for Aerospace Engineering, 2012, 31: 1110–1114 (in Chinese)
7. Wang T, Liu S, Shao J, Li Y. Health monitoring of bolted joints using the time reversal method and piezoelectric transducers. Smart Materials and Structures, 2016, 25(2): 025010
8. Yin H, Wang T, Yang D, Liu S, Shao J, Li Y. A smart washer for bolt looseness monitoring based on piezoelectric active sensing method. Applied Sciences, 2016, 6(11): 320
9. Wu H, Guo Y, Xiong L, Liu W, Li G, Zhou X. Optical fiber-based sensing, measuring, and implementation methods for slope deformation monitoring: A review. IEEE Sensors Journal, 2019, 19(8): 2786–2800
10. Wang P, Zhang N, Kan J, Xie Z, Wei Q, Yao W. Fiber Bragg grating monitoring of full-bolt axial force of the bolt in the deep strong mining roadway. Sensors, 2020, 20(15): 4242
11. Khomenko A, Koricho E, Haq M, Cloud G L. Bolt tension monitoring with reusable fiber Bragg-grating sensors. Journal of Strain Analysis for Engineering Design, 2016, 51(2): 101–108
12. Deng S, Wang T, Tan B, Yu W, Lu G. Proof-of-concept study of bolt connection status monitoring using fiber Bragg grating curvature sensor. Smart Materials and Structures, 2022, 31(11): 114001
13. Chen L, Xiong H, Yang Z, Long Y, Ding Y, Kong Q. Preload measurement of steel-to-timber bolted joint using piezoceramic-based electromechanical impedance method. Measurement, 2022, 190: 110725
14. Wang T, Yang Z, Shao J, Li Y. Research on bolt loosen detection based on piezoelectric impedance technology. Chinese Journal of Sensors and Actuators, 2014, 27(10): 1321–1325 (in Chinese)
15. Balavalad K B. A review on silicon nanowires and their use in the development of nano piezoresistive pressure sensors. Nanoscience & Nanotechnology-Asia, 2023, 13(5): 14–22
16. Nguyen T, Dinh T, Phan H P, Pham T A, Dau V T, Nguyen N T, Dao D V. Advances in ultrasensitive piezoresistive sensors: From conventional to flexible and stretchable applications. Materials Horizons, 2021, 8(8): 2123–2150
17. Wang T, Wei D, Shao J, Li Y, Song G. Structural stress monitoring based on piezoelectric impedance frequency shift. Journal of Aerospace Engineering, 2018, 31(6): 04018092
18. Shao J, Wang T, Yin H, Yang D, Li Y. Bolt looseness detection based on piezoelectric impedance frequency shift. Applied Sciences, 2016, 6(10): 298
19. Wang B, Huo L, Chen D, Li W, Song G. Impedance-based pre-stress monitoring of rock bolts using a piezoceramic-based smart washer—A feasibility study. Sensors, 2017, 17(2): 250
20. Jiang X, Ma K, Lu S, Zhang L, Wang Z, Guo Y, Wang X, Zhao Z, Qu X, Lu Y. Structure bolt tightening force and loosening monitoring by conductive MXene/FPC pressure sensor with high sensitivity and wide sensing range. Sensors and Actuators. A, Physical, 2021, 331: 113005
21. Brøns M, Ebbehøj L, Tcherniak D, Thomsen J J. Using piezoelectrically excited transverse vibrations for bolt tension estimation. In: Proceedings of ISMA 2020 and USD 2020. Red Hook, NY: Curran Associates, Inc., 2020, 1175–1187
22. Pan Q, Pan R, Shao C, Chang M, Xu X. Research review of principles and methods for ultrasonic measurement of axial stress in bolts. Chinese Journal of Mechanical Engineering, 2020, 33(1): 11
23. Li X, Wang S, Li Z, Yang R, Li Z. Measurement of bolt axial stress using a combination of trailing wave and shear wave ultrasound. NDT & E International, 2024, 143: 103056
24. Bickford J. An Introduction to the Design and Behavior of Bolted Joints, Revised and Expanded. New York: Routledge, 2018
25. Koshti A M. Ultrasonic Measurement of Loads in Bolts Used in Structural Joints. NESC NDE IDT Face to Face Meeting Technical Report No. JSC-CN-32910. 2015
26. Amerini F, Meo M. Structural health monitoring of bolted joints using linear and nonlinear acoustic/ultrasound methods. Structural Health Monitoring, 2011, 10(6): 659–672
27. Wang C, Wang N, Ho S, Chen X, Pan M, Song G. Design of a novel wearable sensor device for real-time bolted joints health monitoring. IEEE Internet of Things Journal, 2018, 5(6): 5307–5316
28. Li S, Li H, Zhou X, Wang Y H, Li X H, Gan D, Zhu R H. Damage detection of flange bolts in wind turbine towers using dynamic strain responses. Journal of Civil Structural Health Monitoring, 2023, 13(1): 67–81
29. Miao R, Shen R, Zhang S, Xue S. A review of bolt tightening force measurement and loosening detection. Sensors, 2020, 20(11): 3165
30. Pan Y, Ma Y, Dong Y, Gu Z, Wang D. A vision-based monitoring method for the looseness of high-strength bolt. IEEE Transactions on Instrumentation and Measurement, 2021, 70: 1–14
31. Yang Z, Huo L. Bolt preload monitoring based on percussion sound signal and convolutional neural network (CNN). Nondestructive Testing and Evaluation, 2022, 37(4): 464–481
32. Yuan C, Chen W, Hao H, Kong Q. Near real-time bolt-loosening detection using mask and region-based convolutional neural network. Structural Control and Health Monitoring, 2021, 28(7): e2741
33. Xu J, Dong J, Li H, Zhang C, Ho S C. Looseness monitoring of bolted spherical joint connection using electro-mechanical impedance technique and BP neural networks. Sensors, 2019, 19(8): 1906
34. Baptista F G, Budoya D E, de Almeida V A D, Ulson J A C. An experimental study on the effect of temperature on piezoelectric sensors for impedance-based structural health monitoring. Sensors, 2014, 14(1): 1208–1227